NACA

RESEARCH MEMORANDUM

LOW-SPEED INVESTIGATION OF THE AERODYNAMIC, CONTROL, AND HINGE-MOMENT CHARACTERISTICS IN SIDESLIP OF A DELTA-WING—FUSELAGE MODEL WITH HORN-BALANCE TYPE AILERONS AND WITH AND WITHOUT NACELLES

By William I. Scallion

Langley Aeronautical Laboratory
Langley Field, Va.

NATIONAL ADVISORY COMMITTEE
FOR AERONAUTICS

WASHINGTON
August 21, 1953

NATIONAL ADVISORY COMMITTEE FOR AERONAUTICS

RESEARCH MEMORANDUM

LOW-SPEED INVESTIGATION OF THE AERODYNAMIC, CONTROL, AND HINGE-MOMENT CHARACTERISTICS IN SIDESLIP OF A DELTA-WING—FUSELAGE MODEL WITH HORN-BALANCE-TYPE AILERONS AND WITH AND WITHOUT NACELLES

By William I. Scallion

SUMMARY

An investigation was made in the Langley full-scale tunnel to determine the low-speed aerodynamic, control, and control hinge-moment characteristics of a 3-percent-thick, tailless, delta-wing—fuselage combination in sideslip. The model had horn-balance-type ailerons of 10.2-percent total wing area and was tested with and without chord-plane nacelles mounted at the 0.48-semispan station. Aerodynamic forces and moments and hinge-moment data were obtained through the angle-of-attack range of -3.7° to 36.3° at a Reynolds number of 2.3×10^{6} and a Mach number of 0.10.

The model without nacelles was directionally unstable at all lift coefficients and had positive effective dihedral throughout the lift range tested. The nacelles improved the directional stability characteristics of the model at high lift coefficients, but there was a sharp increase in directional instability at maximum lift. The nacelles increased the effective dihedral at all lift coefficients. The variation of sideslip angles up to 9.7° did not affect the control effectiveness of the ailerons or the yawing moments due to aileron deflection. The rate of change of hinge-moment coefficient with aileron deflection of the advanced wing aileron was reduced with increasing sideslip but that of the retarded wing aileron was relatively unaffected by sideslip.

INTRODUCTION

The determination of the low-speed lateral stability and control characteristics of delta wings has been the objective of many investigations in which a variety of configurations and types of controls were

tested; however, the effects of sideslip on the lateral control and control hinge-moment characteristics have not been extensively studied. In addition, there is little information on the effects of chord-plane mounted nacelles on the lateral stability and control characteristics of delta wings in sideslip which, therefore, merits study in view of the influence of such nacelles on the low-speed stall characteristics as indicated by reference 1.

As part of a program of the investigation of the low-speed aerodynamic and control characteristics of thin delta wings in the Langley full-scale tunnel, the tests reported herein were made on a 3-percent-thick, 60°-sweptback-delta-wing–fuselage combination at several angles of sideslip. These tests included the lateral stability characteristics of the model with and without nacelles mounted on the wing-chord plane at the 0.48-semispan station. In addition, the effects of sideslip on the control and hinge-moment characteristics of horn-balance-type tip ailerons of 10.2 percent total wing area were investigated on the model with and without the nacelles installed. Forces and moments, as well as hinge-moment data, were obtained in the angle-of-attack range of -3.7° through the angle for maximum lift. The test Reynolds number was 2.3×10^6 and the Mach number was 0.10. In order to expedite publication, the data have been presented without detailed analysis.

COEFFICIENTS AND SYMBOLS

All results are presented in standard NACA form of coefficients of forces and moments. The wing moments are referred to the stability axes originating at the projection of the quarter-point of the mean aerodynamic chord on the plane of symmetry. The positive directions of forces, moments, and angles are shown in figure 1. The coefficients and symbols are defined as follows:

C_L lift coefficient, L/qS

C_X longitudinal-force coefficient, X/qS

C_Y lateral-force coefficient, Y/qS

C_m pitching-moment coefficient, $M/qS\bar{c}$

C_n yawing-moment coefficient, N/qSb

C_l rolling-moment coefficient, L'/qSb

C_h hinge-moment coefficient, $H/2qQ$

L lift, lb

X longitudinal force, lb

Y lateral force, lb

M pitching moment, ft-lb

N yawing moment, ft-lb

L' rolling moment, ft-lb

H hinge moment, ft-lb

ρ mass density of air, slugs/cu ft

q free-stream dynamic pressure, $\rho V^2/2$, lb/sq ft

V free-stream velocity, ft/sec

S total wing area, sq ft

Q moment of area of control surface rearward of hinge line about hinge line, ft^3

$\bar{c}$ wing mean aerodynamic chord measured parallel to plane of symmetry, $2/S \int_0^{b/2} c^2 \, dy$, ft

c wing chord measured parallel to plane of symmetry, ft

b wing span, ft

y distance along lateral axis, ft

α angle of attack of wing chord line, deg

β angle of sideslip, deg

δ control deflection, deg

C_{Y_β} rate of change of lateral-force coefficient with angle of sideslip (slope at zero sideslip), per deg

C_{n_β} rate of change of yawing-moment coefficient with angle of sideslip (slope at zero sideslip), per deg

C_{l_β} rate of change of rolling-moment coefficient with angle of sideslip (slope at zero sideslip), per deg

C_{n_δ} rate of change of yawing-moment coefficient with control deflection (slope at zero deflection), per deg

C_{l_δ} rate of change of rolling-moment coefficient with control deflection (slope at zero deflection), per deg

C_{h_δ} rate of change of hinge-moment coefficient with control deflection (slope at zero deflection), per deg

Subscripts:

r right, facing forward

l left, facing forward

MODEL AND TESTS

The model in this investigation had a delta-plan-form wing with the leading edge swept back 60°, an aspect ratio of 2.31, and NACA 65A003 airfoil sections parallel to the model axis of symmetry. The wing was symmetrically located on the fuselage with the $0.25\bar{c}$ point on the wing $0.17\bar{c}$ behind the maximum thickness station of the fuselage. Coordinates for the fuselage, nacelle, and wing section are given in tables I and II. The configuration was tested without vertical surfaces. The general arrangement of the model, controls, and nacelles are given in figure 2. As shown in this figure, the nacelles were symmetrically mounted on the wing-chord plane at the 0.48-semispan station.

The controls were the horn-balance type with the total control area 10.2 percent of the total wing area and with the hinge line located at 0.88 wing-root chord. The balance area ahead of the hinge line was 14 percent of the total control area. The controls were deflected as ailerons ($\delta_r = -\delta_l$) for deflection angles of -30°, -20°, -10°, 0°, 10°, 20°, and 30° and were tested with and without nacelles installed.

The model was tested at angles of attack ranging from -3.7° to 36.3° and at sideslip angles of -2.3°, 0°, 1.7°, 4.9°, 9.7°, and 14.9°. Aerodynamic forces, moments, and hinge moments were obtained by use of a six-component strain-gage balance in the fuselage and strain-gage beams attached to the control surfaces. The model was mounted on a sting

support for tests in the Langley full-scale tunnel as shown in figure 3. The test Reynolds number was 2.3×10^6 based on the mean aerodynamic chord and the Mach number was 0.10. The data have been corrected for jet blockage and an average stream angle of 0.3°. Calculations were made to determine the jet-boundary correction (by method of ref. 2) and buoyancy correction but they were found to be negligible and, therefore, were not applied.

PRESENTATION OF RESULTS

The basic longitudinal characteristics, C_L against α, C_X against C_L, and C_m against C_L, at several sideslip angles of the model with and without nacelles, are shown in figure 4. The effects of the nacelles on the longitudinal characteristics at zero sideslip have been reported in reference 1. The variation of C_Y, C_n, and C_l with angle of attack at several angles of sideslip for the model with and without nacelles is shown in figure 5. Figure 6 shows the effect of sideslip on the lateral aerodynamic characteristics (C_Y, C_n, and C_l) at several angles of attack. Figures 7 and 8 show the effects of deflecting the horn-balance-type ailerons on the yawing-moment and rolling-moment coefficients at $\beta = 0°$, 4.9°, and 9.7° for most of the angle-of-attack range. In order to give a more complete account of the effects of sideslip on the variation of C_h with α for the horn-balance-type ailerons on the model with and without the nacelles installed, the hinge-moment coefficients of both ailerons were recorded when the model was tested in sideslip and are shown in figure 9. The variation of C_h with δ for both the right and left ailerons for several angles of attack and at sideslip angles of 0°, 4.9°, and 9.7° are given in figure 10.

In order to present the static lateral stability, control, and control hinge-moment characteristics in a more useful form for comparative purposes, summary plots are presented in figures 11 and 12. Although a detailed analysis is beyond the intended scope of this paper, some of the more pertinent results as shown by the summary figures are noted as follows.

As shown in figure 11 the model without nacelles is directionally unstable (negative C_{n_β}) throughout the lift range as might be expected with a wing fuselage without a vertical tail. (See ref. 3.) The degree of instability increases sharply above $C_L = 0.8$ to $C_{n_\beta} = -0.0041$ at maximum lift. The dihedral parameter C_{l_β} is negative at all positive lift coefficients (positive effective dihedral) and increases to a maximum value at $C_L = 0.6$. Above this lift coefficient, the effects of

separation on the advanced wing cause C_{l_β} to decrease to a minimum value just prior to maximum lift.

With the nacelles installed, the directional instability was reduced to zero or neutral stability at $C_L = 0.8$, but there was a sharp unstable break at maximum lift. The effect of the nacelles on C_{l_β} is to increase the effective dihedral throughout the lift-coefficient range with an abrupt increase in C_{l_β} at maximum lift.

From the lateral control and control hinge-moment data of figure 12, it is found that the control effectiveness of the horn-balance-type ailerons is not materially influenced by sideslip angles up to 9.7° but is increased by installation of the nacelles as previously shown by reference 4. The adverse yawing moments due to control deflection (positive C_{n_δ}) are relatively unaffected by either sideslip or the nacelles throughout the C_L range.

The value of the aileron hinge-moment parameter C_{h_δ} is fairly large at all lift coefficients, and installation of the nacelles tends to increase the value of C_{h_δ}. Increasing sideslip reduces the value of C_{h_δ} for the advanced wing aileron, but the hinge-moment characteristics of the retarded wing aileron are not materially affected by sideslip.

SUMMARY OF RESULTS

The results of the low-speed investigation of the aerodynamic, control, and control hinge-moment characteristics in sideslip of a 3-percent-thick, tailless, 60°-sweptback-delta-wing—fuselage combination with horn-balance-type ailerons of 10.2 percent total wing area and with and without chord-plane nacelles mounted at 0.48-semispan station may be summarized as follows:

1. The wing-fuselage model without nacelles was directionally unstable at all lift coefficients and had positive effective dihedral throughout the lift range, the maximum effective dihedral occurring at a lift coefficient of 0.6.

2. Installation of the nacelles reduced the directional instability of the model at high lift coefficients but there was a sharp unstable break at maximum lift. The nacelles caused increases in the effective dihedral at all lift coefficients.

3. Variation of sideslip angles up to 9.7° had only small effects on the control effectiveness of the ailerons and the yawing moments produced by aileron deflection on the model with and without nacelles.

4. Increasing sideslip reduced the rate of change of hinge-moment coefficient with aileron deflection C_{h_δ} on the advanced wing aileron but had little effect on C_{h_δ} of the retarded wing aileron.

Langley Aeronautical Laboratory,
National Advisory Committee for Aeronautics,
Langley Field, Va., June 23, 1953.

REFERENCES

1. Scallion, William I.: Low-Speed Investigation of the Effects of Nacelles on the Longitudinal Aerodynamic Characteristics of a 60° Sweptback Delta-Wing—Fuselage Combination With NACA 65A003 Airfoil Sections. NACA RM L52F04, 1952.

2. Katzoff, S., and Hannah, Margery E.: Calculation of Tunnel-Induced Upwash Velocities for Swept and Yawed Wings. NACA TN 1748, 1948.

3. Jaquet, Byron M., and Brewer, Jack D.: Effects of Various Outboard and Central Fins on Low-Speed Static-Stability and Rolling Characteristics of a Triangular-Wing Model. NACA RM L9E18, 1949.

4. Scallion, William I : Low-Speed Investigation of the Aerodynamic, Control, and Hinge-Moment Characteristics of Two Types of Controls on a Delta-Wing—Fuselage Model With and Without Nacelles. NACA RM L53C18, 1953.

TABLE I

COORDINATES OF FUSELAGE AND NACELLES

Fuselage ordinates		
Station	x_o, in.	y_o, in.
0	0	0
1	.72	.333
2	1.08	.4284
3	1.80	.6156
4	3.60	1.040
5	7.20	1.735
6	10.80	2.322
7	14.40	2.838
8	21.60	3.733
9	28.80	4.449
10	36.00	4.989
11	43.20	5.387
12	50.40	5.662
13	57.60	5.850
14	64.80	5.965
15	72.00	6.001
16	79.20	5.947
17	86.40	5.794
18	93.60	5.466
19	100.80	5.128
20	108.00	4.789
21	115.20	4.453
22	120.00	4.224
Nose radius = 0.072 in.		

Nacelle ordinates		
Station	x_o, in.	y_o, in.
0	0	0
1	.279	.195
2	.921	.471
3	2.315	.937
4	3.170	1.364
5	5.106	1.735
6	6.500	2.084
7	7.198	2.232
8	8.252	2.444
9	10.002	2.717
10	13.503	3.083
11	17.005	3.320
12	20.51	3.459
13	24.00	3.501
14	46.95	3.501
15	49.86	3.451
16	52.77	3.334
17	55.67	3.144
18	58.58	2.871
19	61.48	2.536
20	64.39	2.142
21	67.29	1.719
22	67.65	1.668
Nose radius = 0.139 in.		

TABLE II

NACA 65A003 AIRFOIL ORDINATES

Station, percent chord	y, percent chord
0	0
.5	.234
.75	.284
1.25	.362
2.50	.493
5.00	.658
7.50	.796
10.00	.912
15.00	1.097
20.00	1.236
25.00	1.342
30.00	1.420
35.00	1.472
40.00	1.498
45.00	1.497
50.00	1.465
55.00	1.402
60.00	1.309
65.00	1.191
70.00	1.053
75.00	.897
80.00	.727
85.00	.549
90.00	.369
95.00	.188
100.00	.007
L.E. radius = 0.058 percent c	

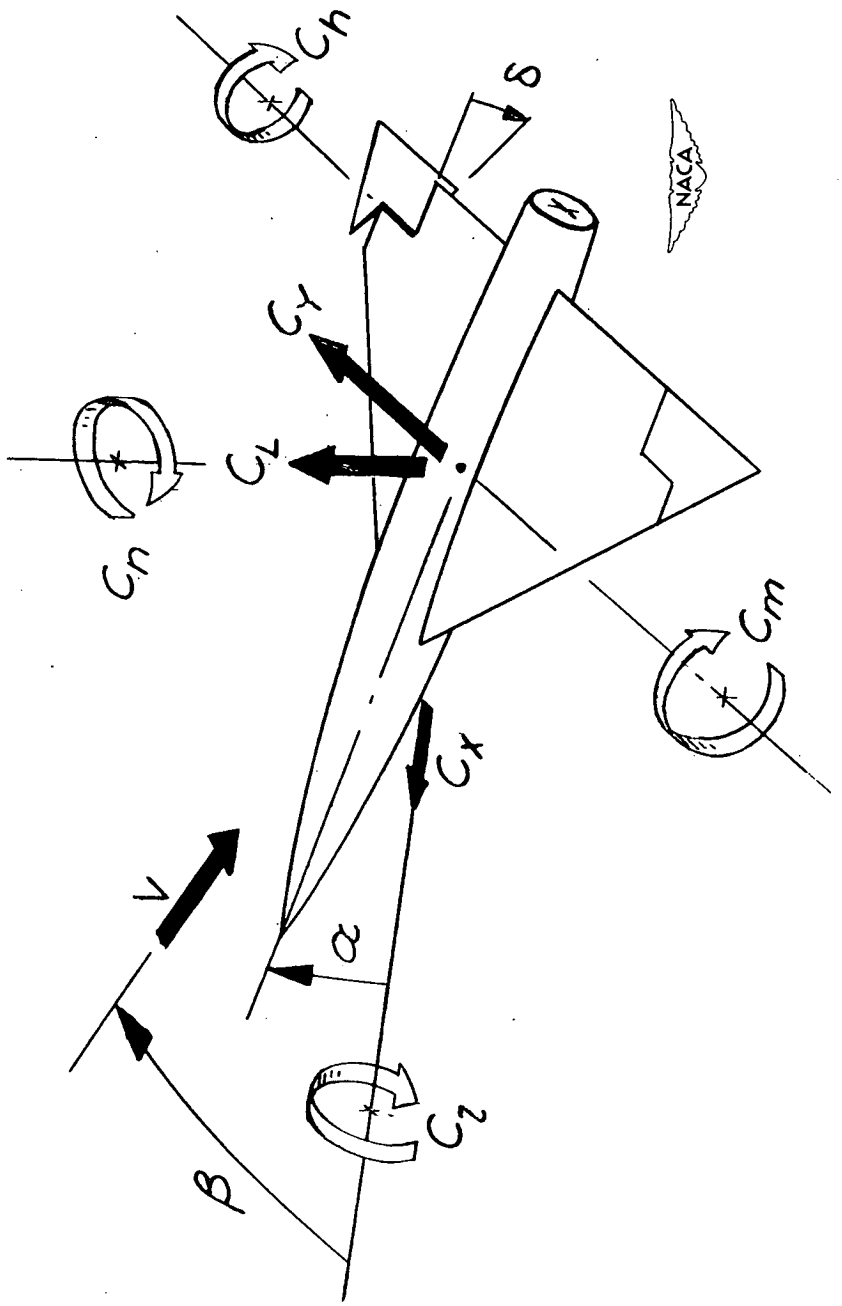

Figure 1.- System of axes used. Arrows indicate positive direction of forces, moments, and angular displacements.

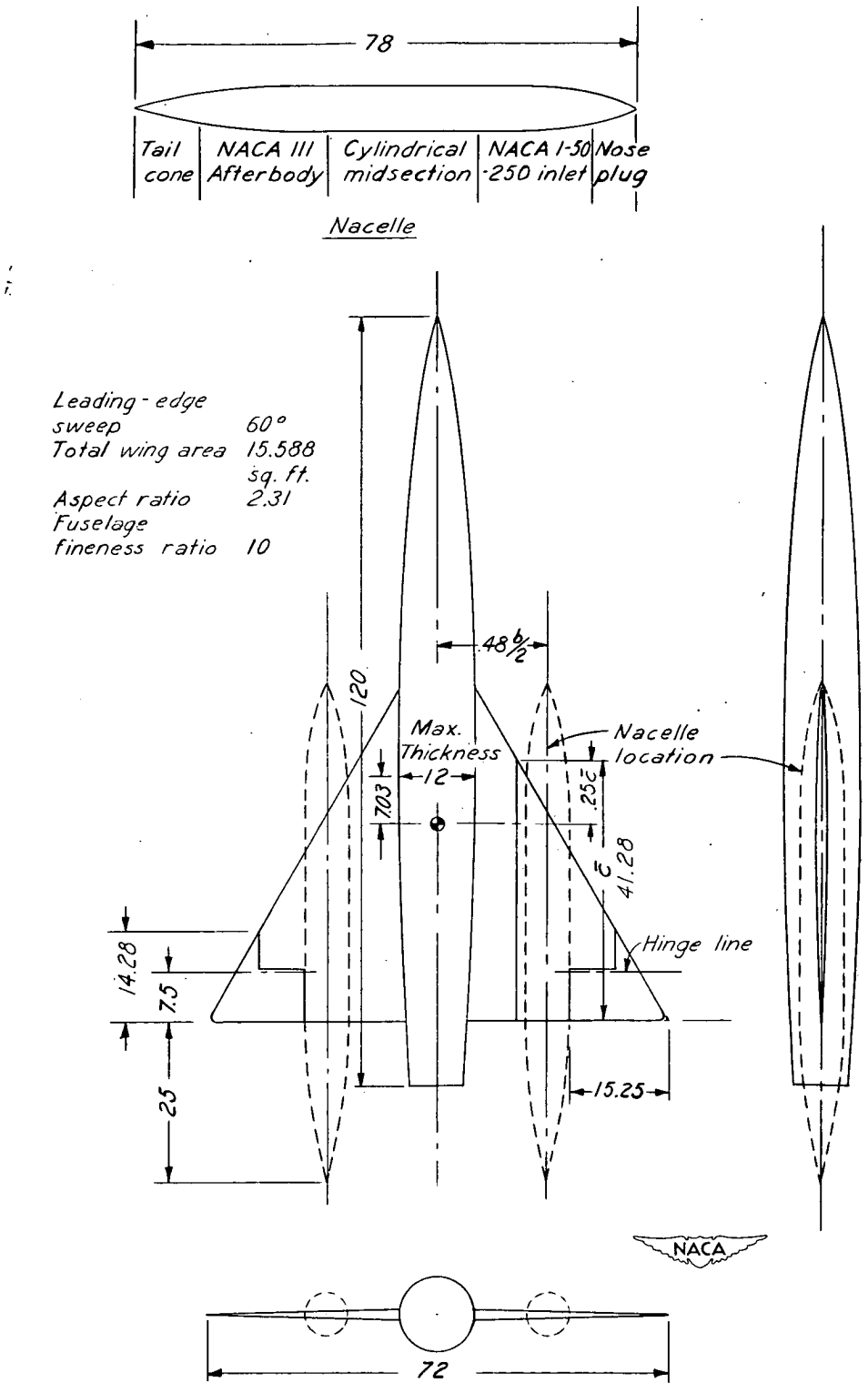

Figure 2.- General arrangement and principal dimensions of the 60° delta-wing model. All dimensions are given in inches.

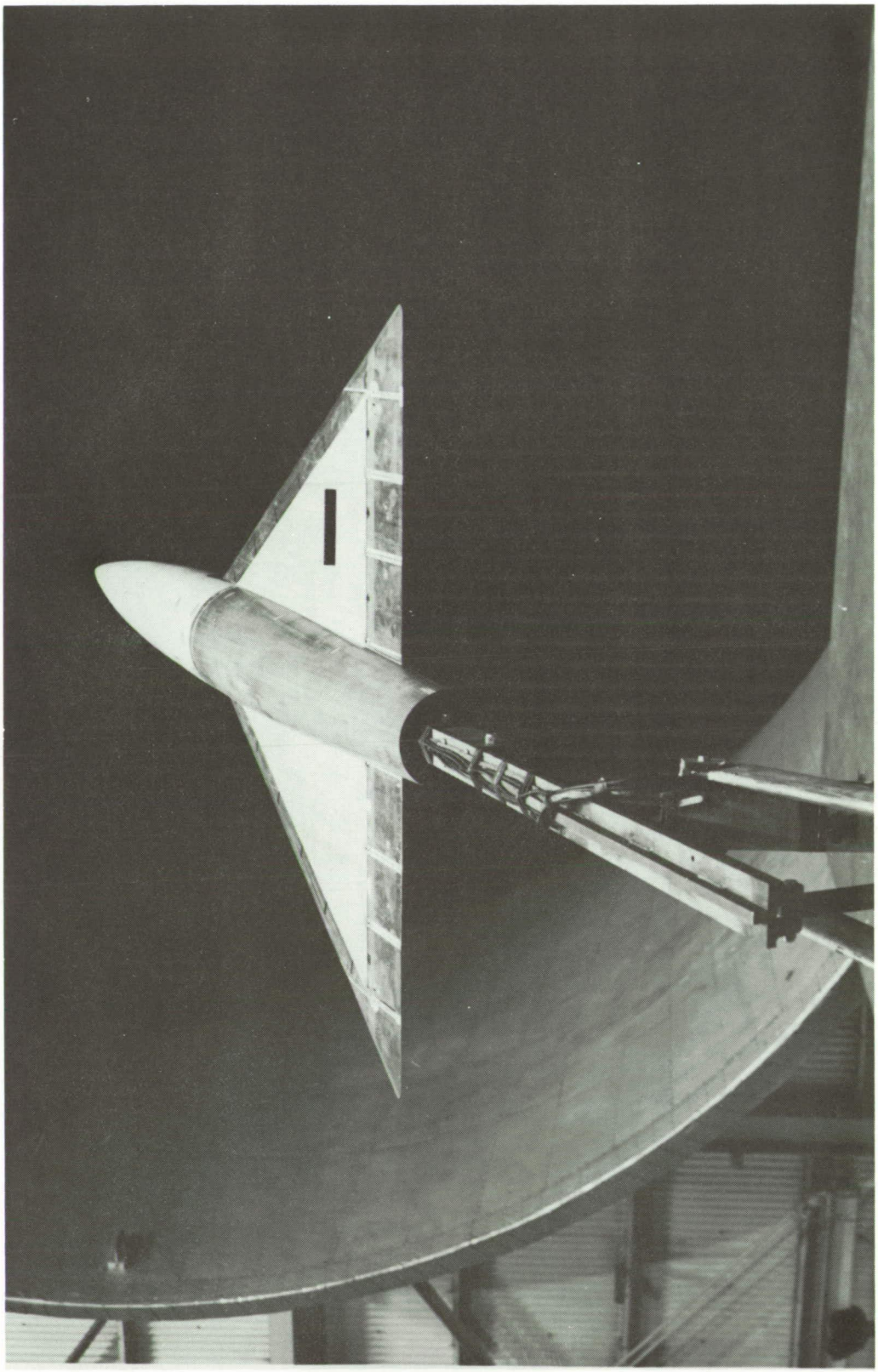

L-76674

Figure 3.- Photograph of the 60° delta-wing model as mounted in the Langley full-scale tunnel.

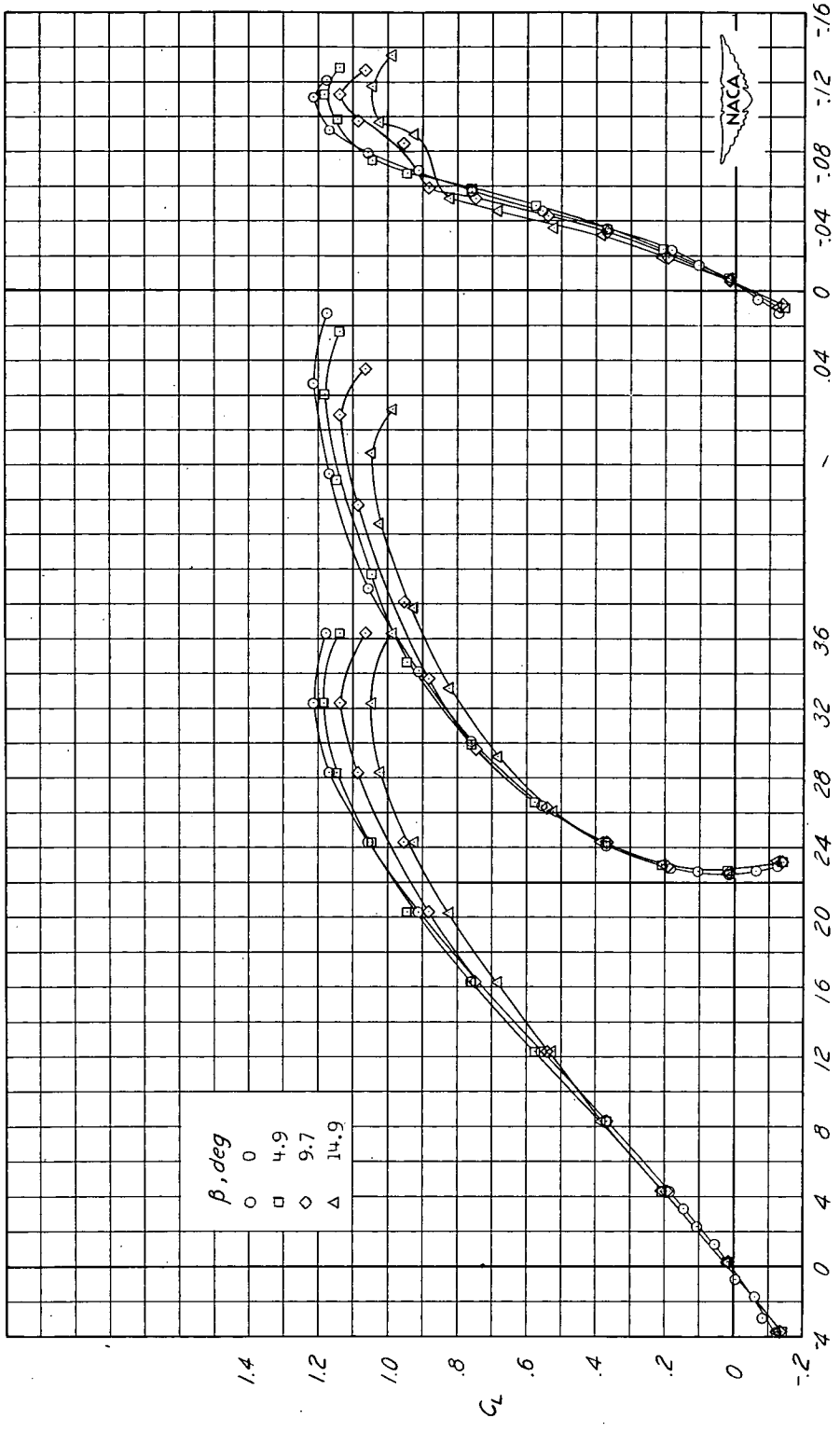

(a) Model without nacelles.

Figure 4.- Longitudinal characteristics of the delta-wing model at several angles of sideslip. $\delta = 0^\circ$.

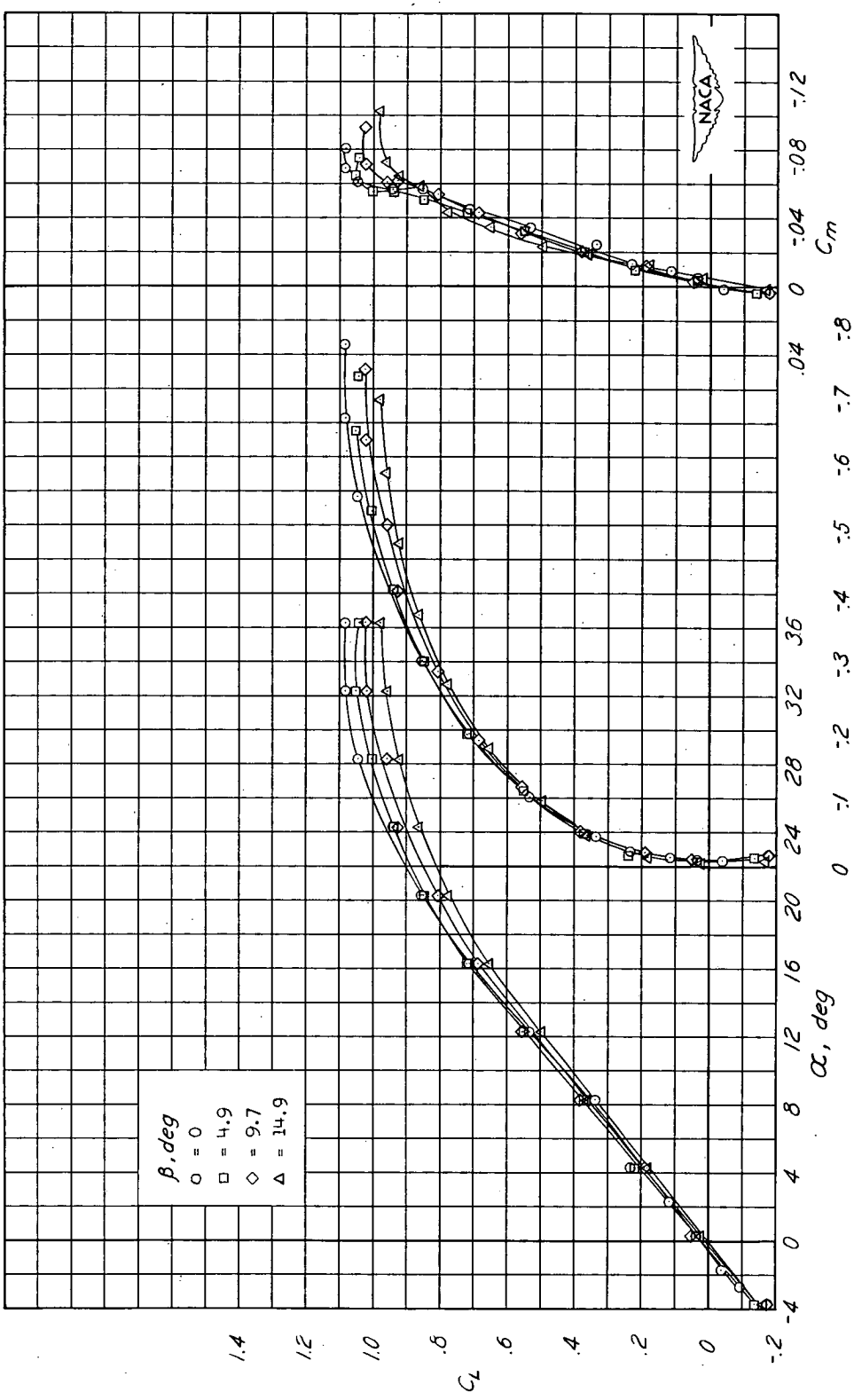

(b) Model with nacelles.

Figure 4.- Concluded.

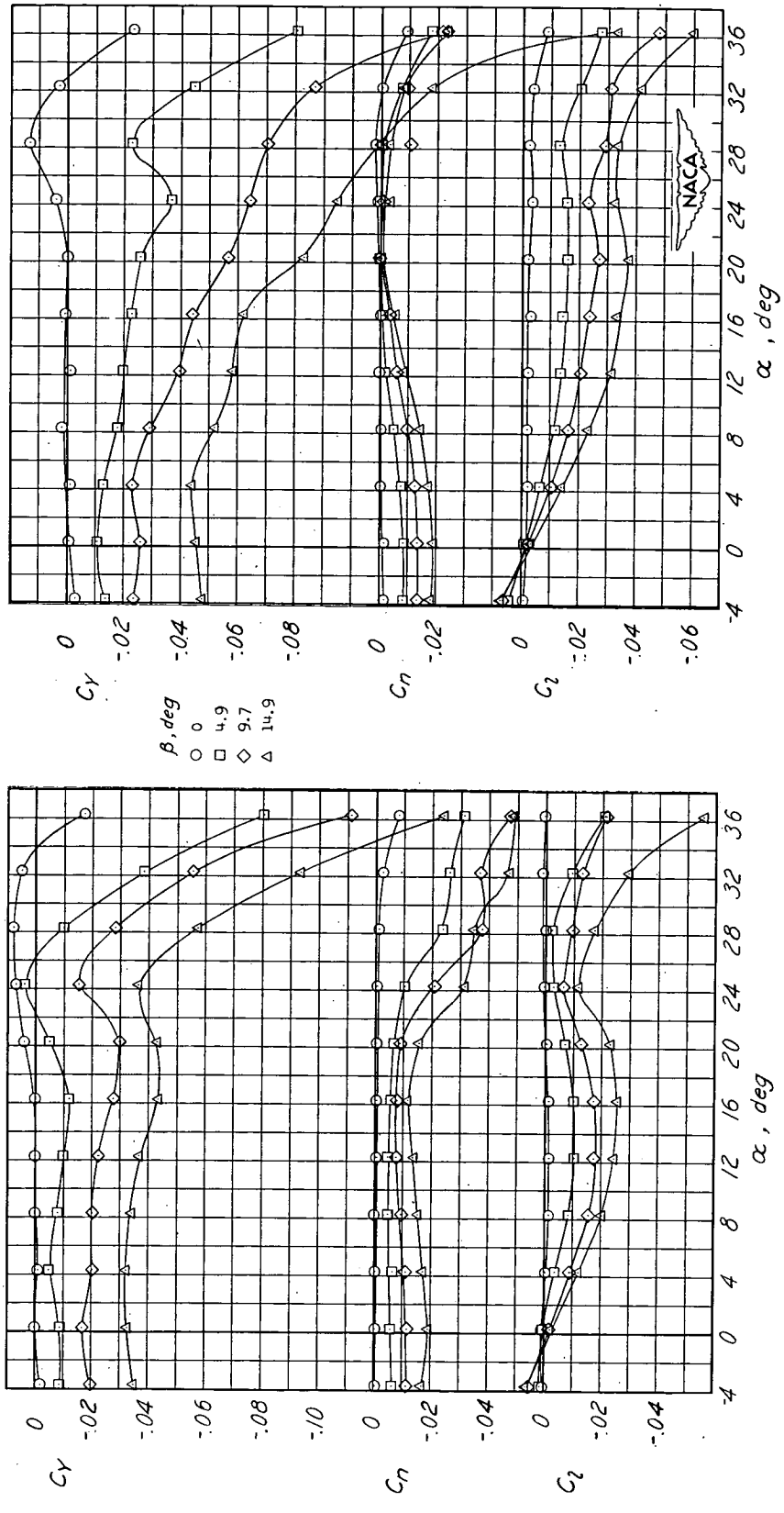

(a) Model without nacelles.

(b) Model with nacelles.

Figure 5.- Effect of sideslip on the variation of lateral-force, yawing-moment, and rolling-moment coefficients with angle of attack. $\delta = 0^\circ$.

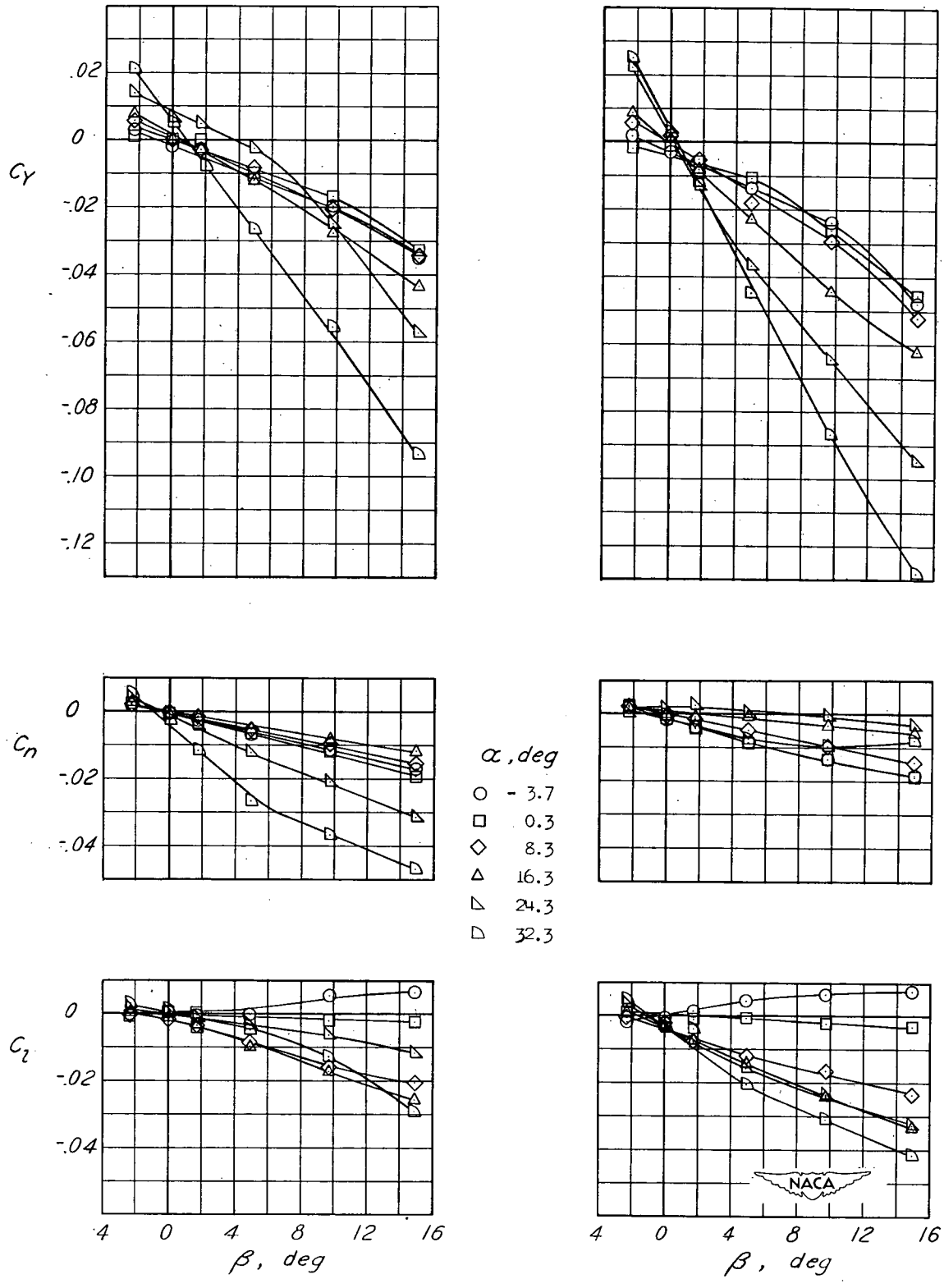

Model without nacelles.

Model with nacelles.

Figure 6.- Lateral and directional characteristics of the delta-wing model at several angles of attack. $\delta = 0^{\circ}$.

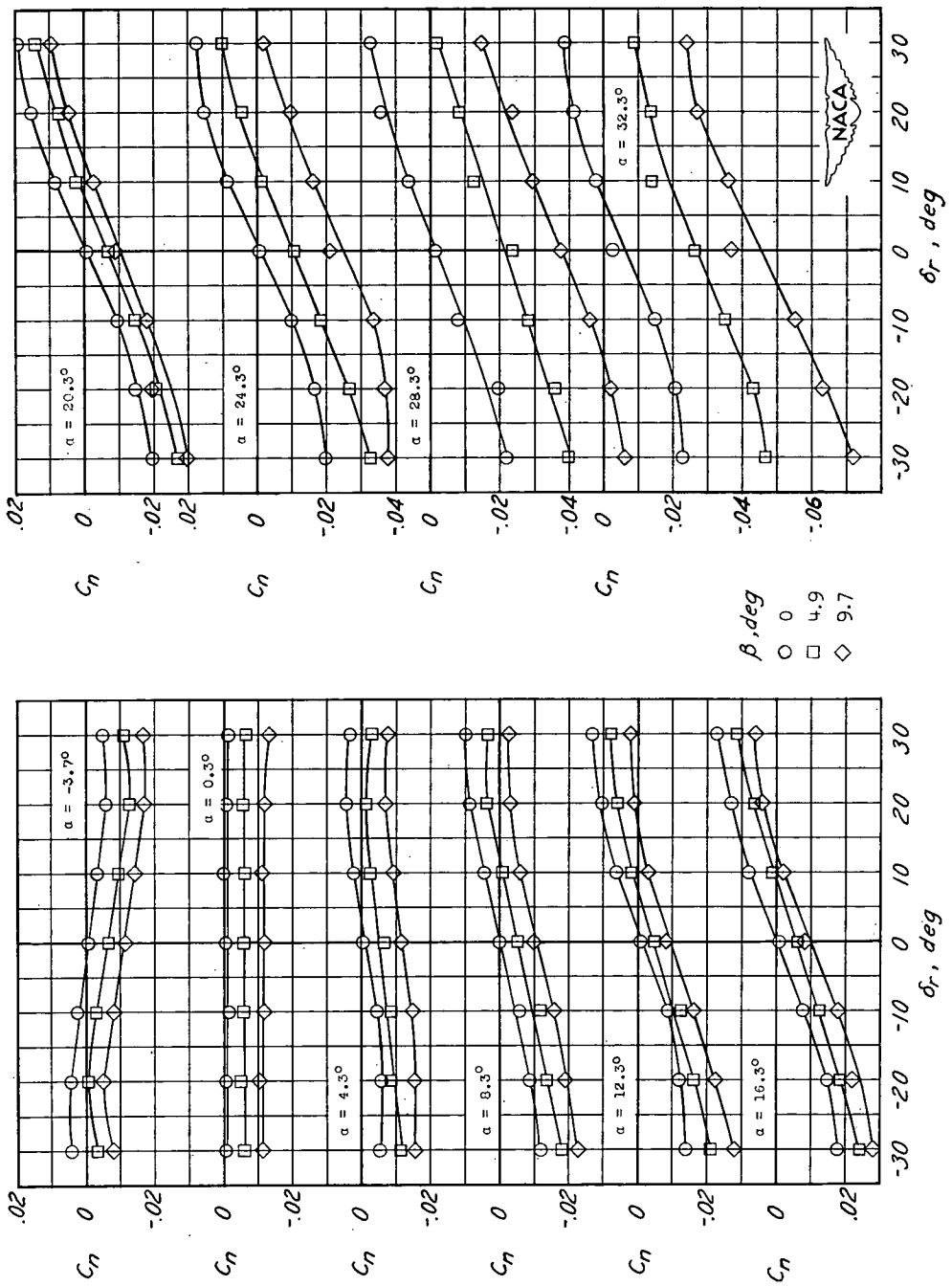

(a) Model without nacelles.

Figure 7.- Variation of yawing-moment coefficient with aileron deflection at several angles of sideslip.

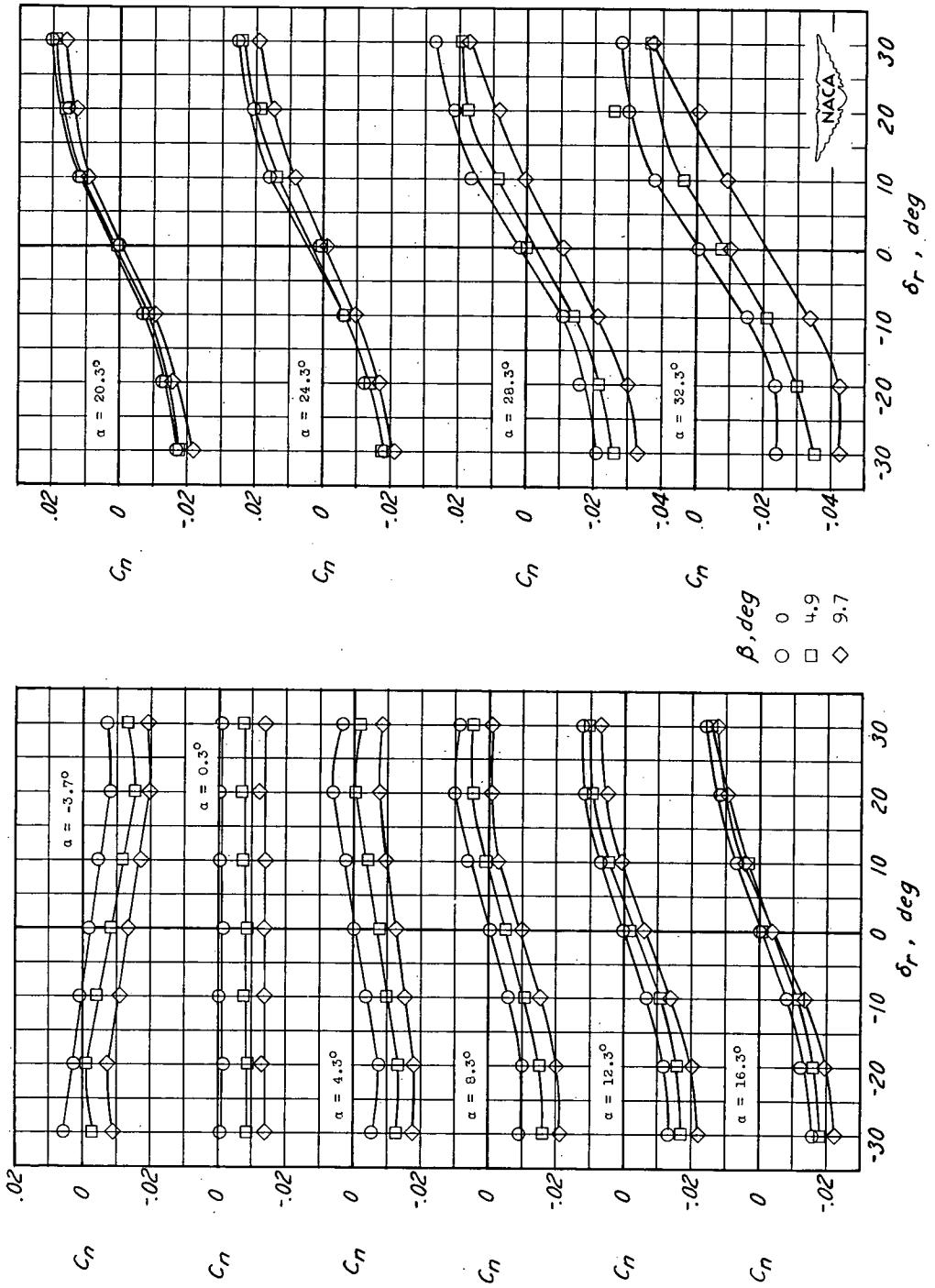

(b) Model with nacelles.

Figure 7.- Concluded.

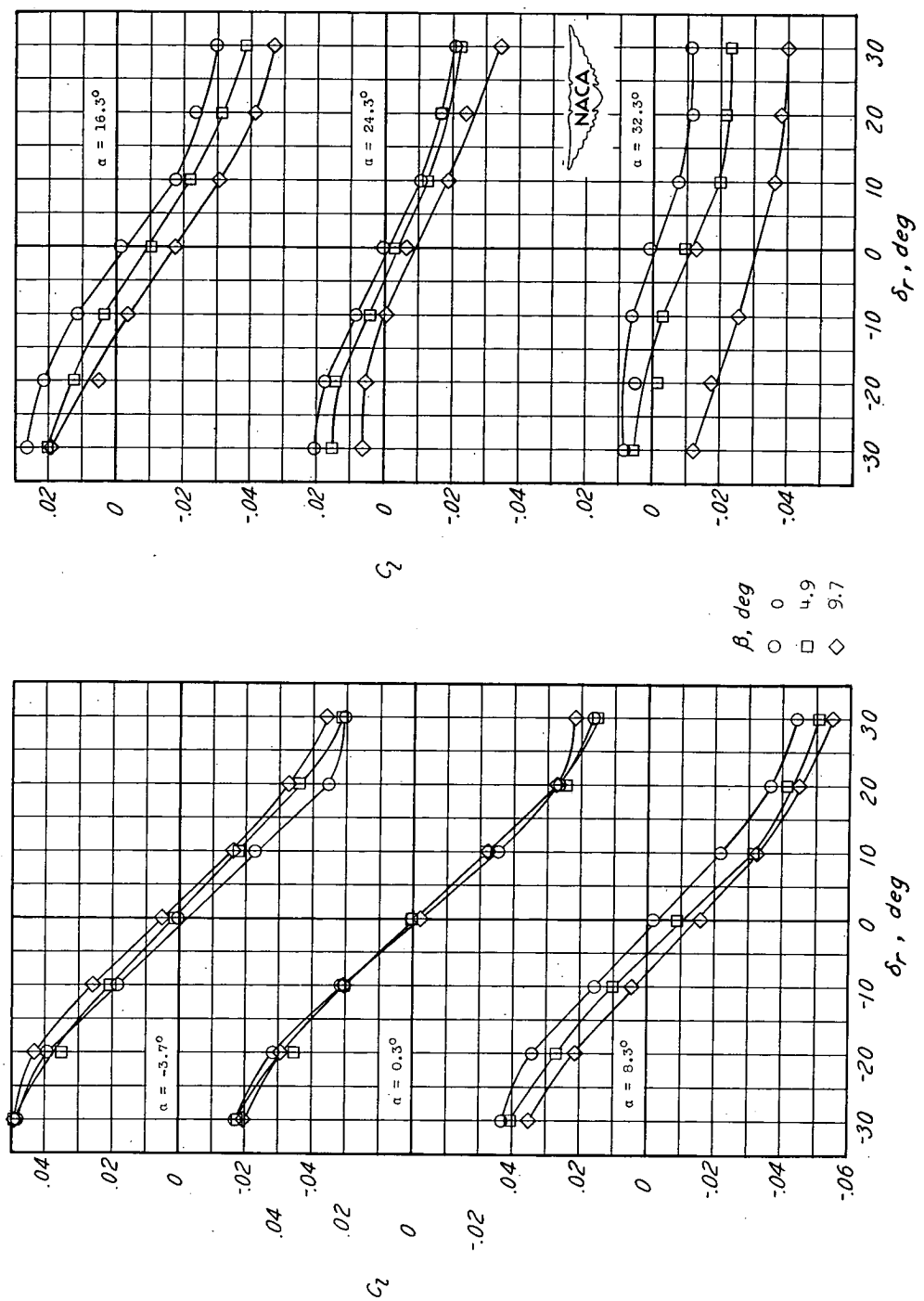

(a) Model without nacelles.

Figure 8.- Variation of rolling-moment coefficient with aileron deflection at several angles of sideslip.

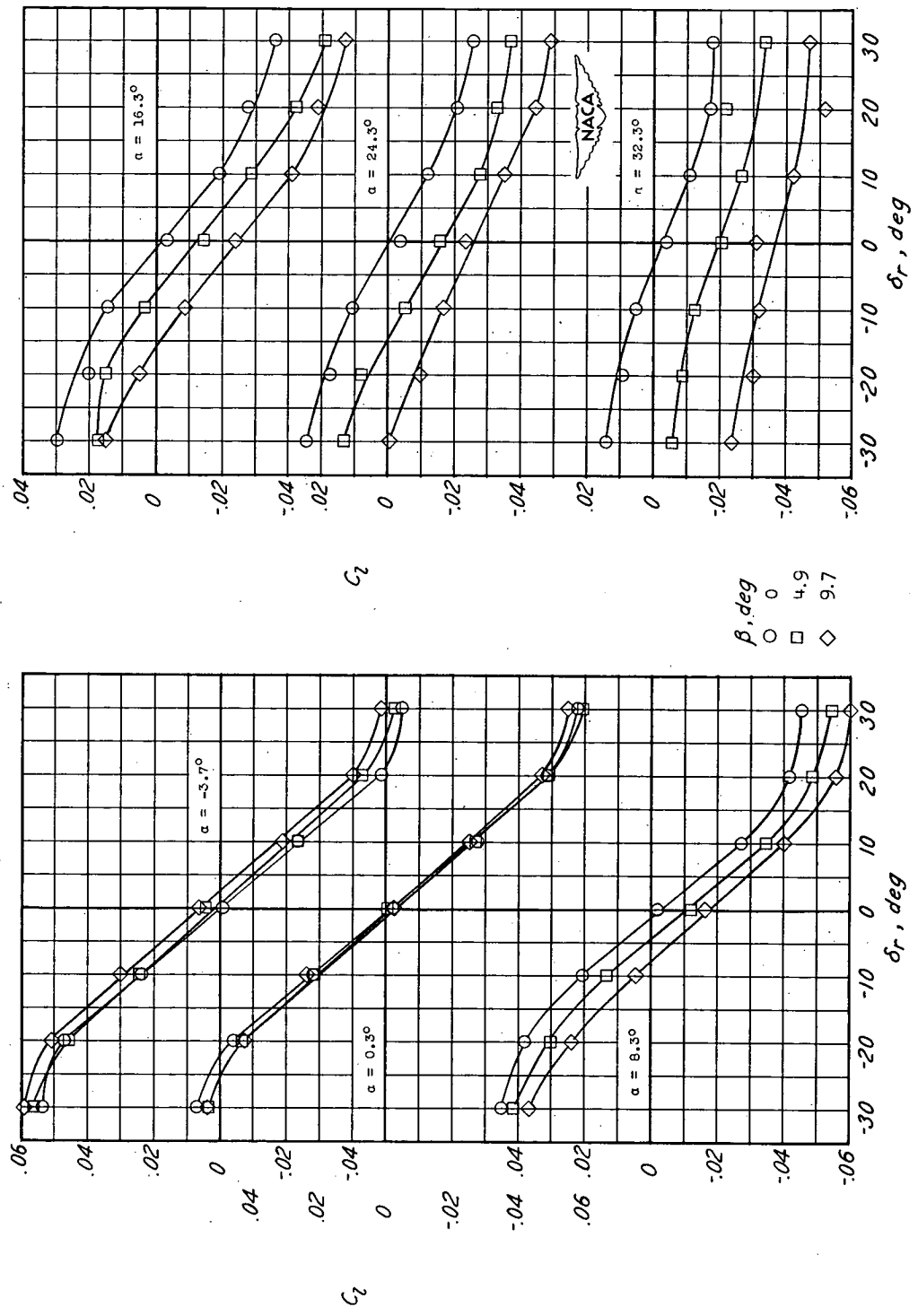

(b) Model with nacelles.

Figure 8.- Concluded.

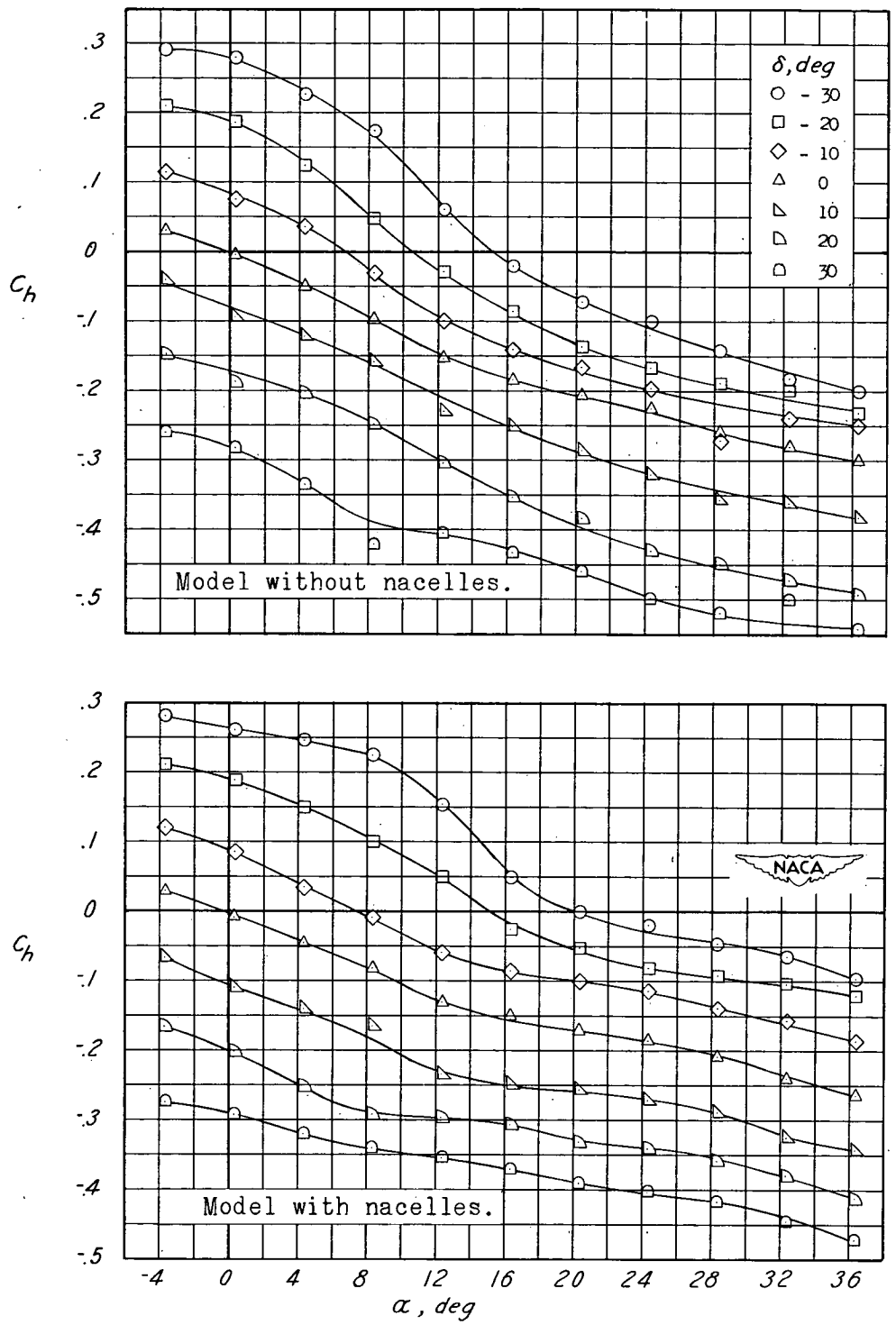

(a) Right aileron, $\beta = 0^{\circ}$.

Figure 9.- Variation of aileron hinge-moment coefficient with angle of attack at several angles of sideslip.

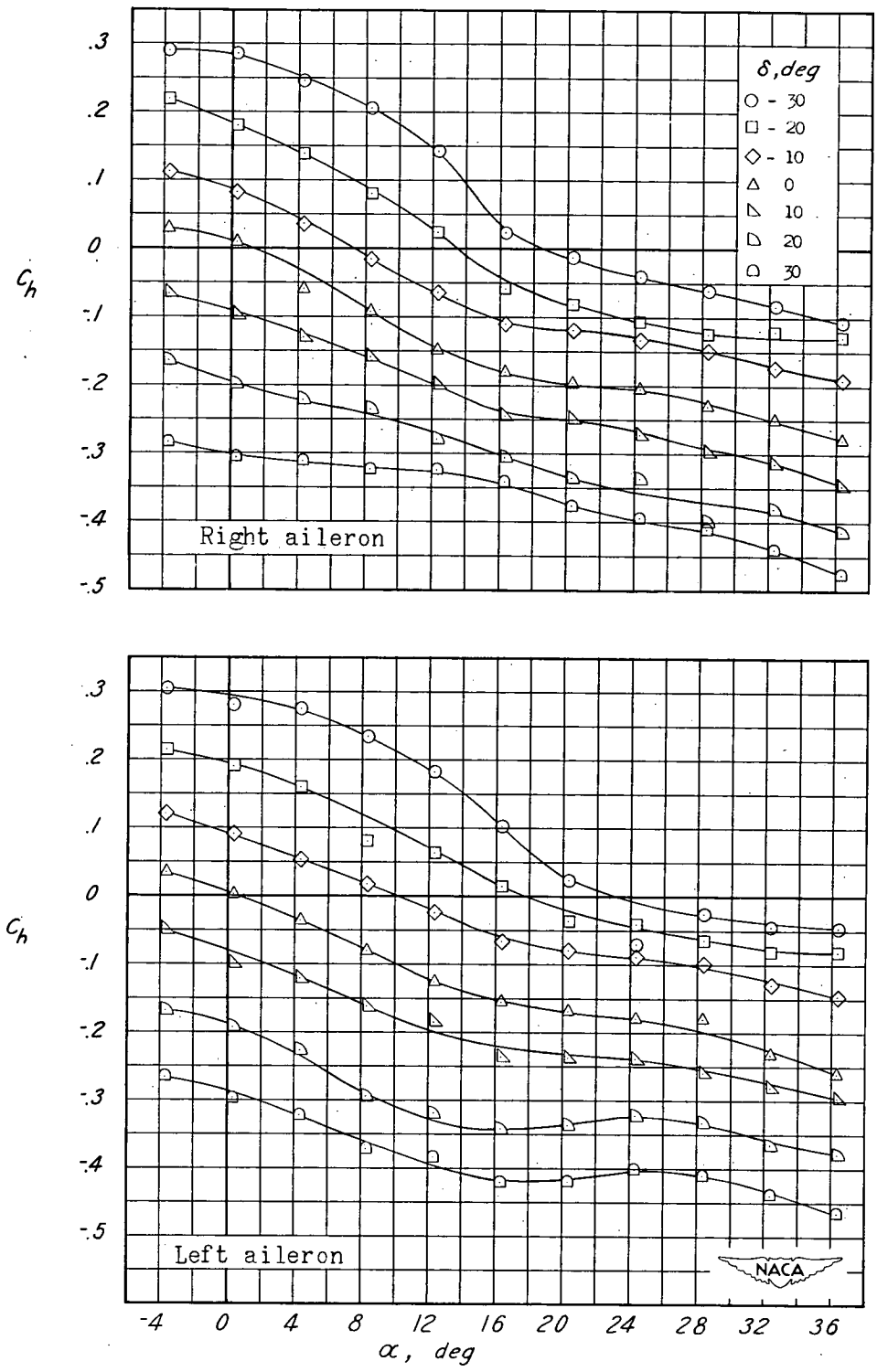

(b) Model without nacelles, $\beta = 4.9^{\circ}$.

Figure 9.- Continued.

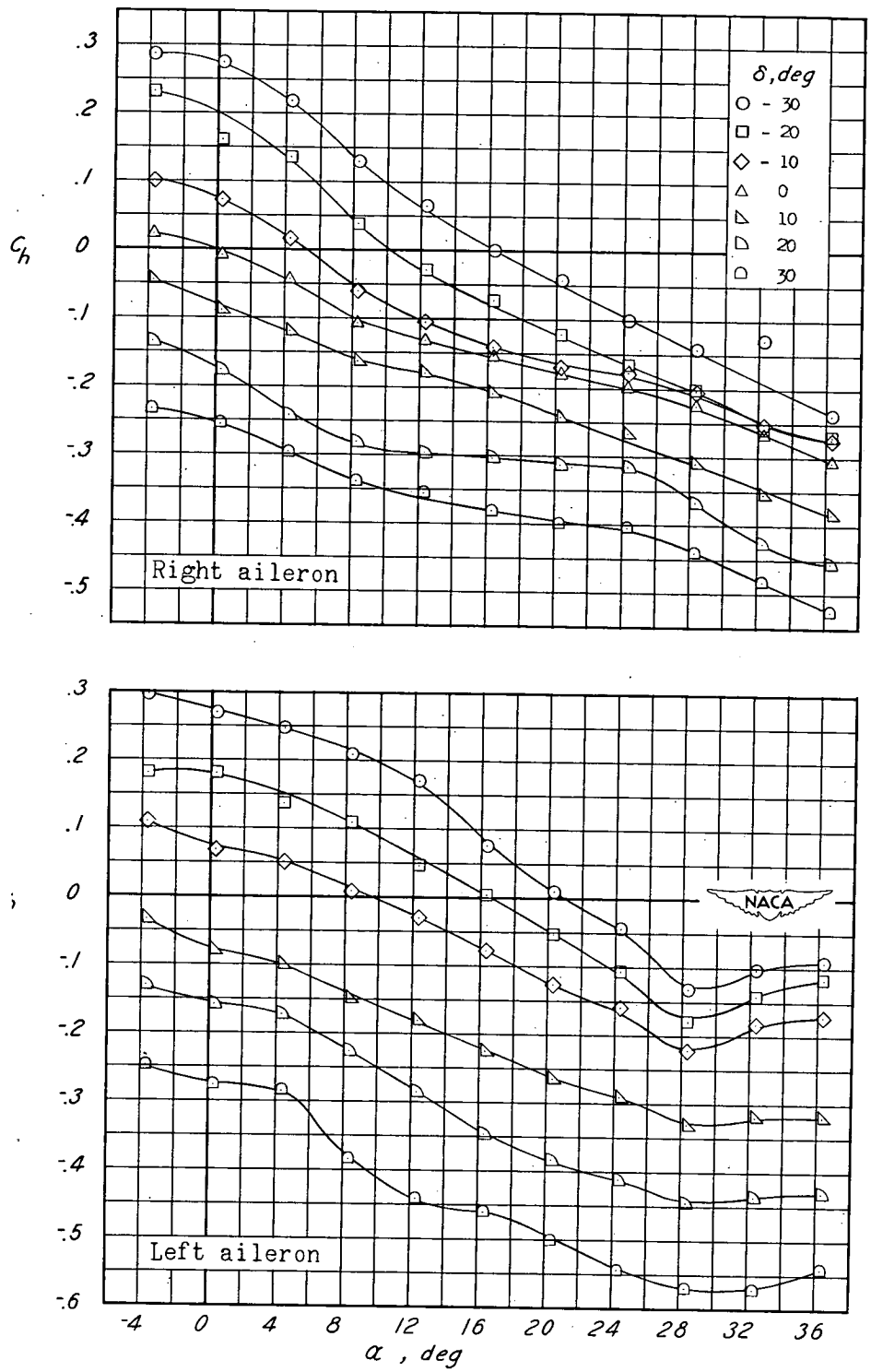

(c) Model without nacelles, $\beta = 9.7^{\circ}$.

Figure 9.- Continued.

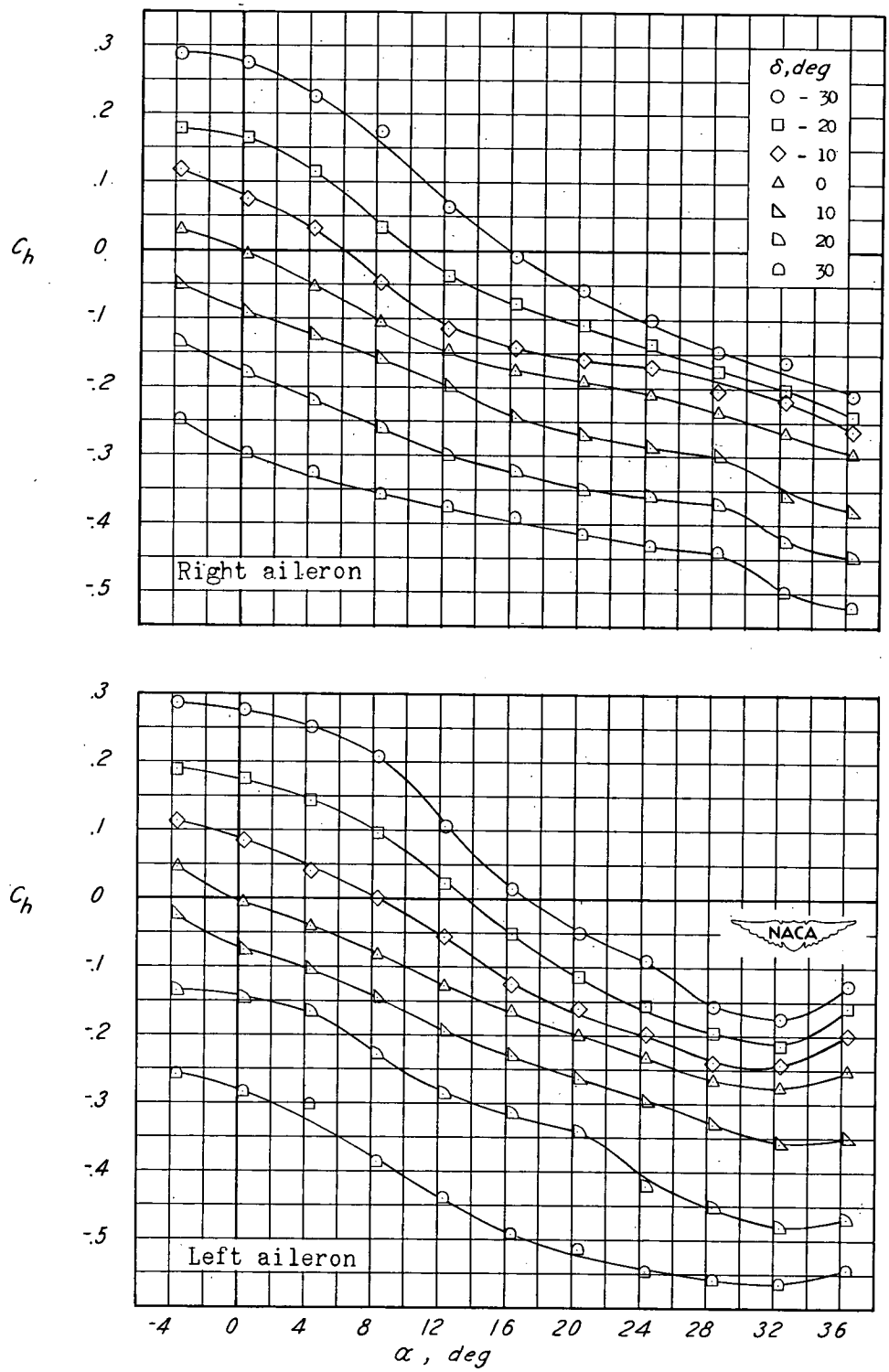

(d) Model with nacelles, $\beta = 4.9^{\circ}$.

Figure 9.- Continued.

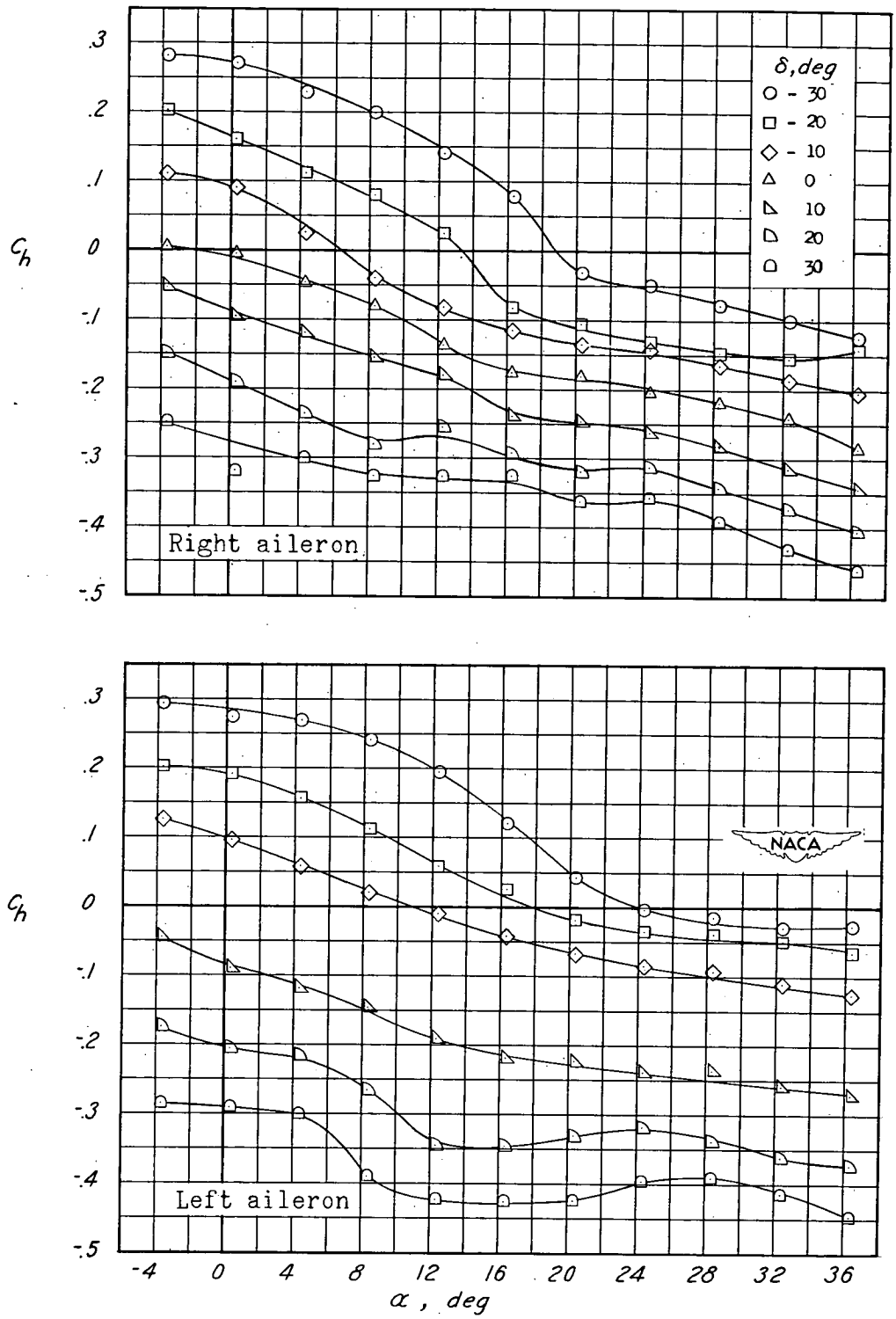

(e) Model with nacelles, $\beta = 9.7^{\circ}$.

Figure 9.- Concluded.

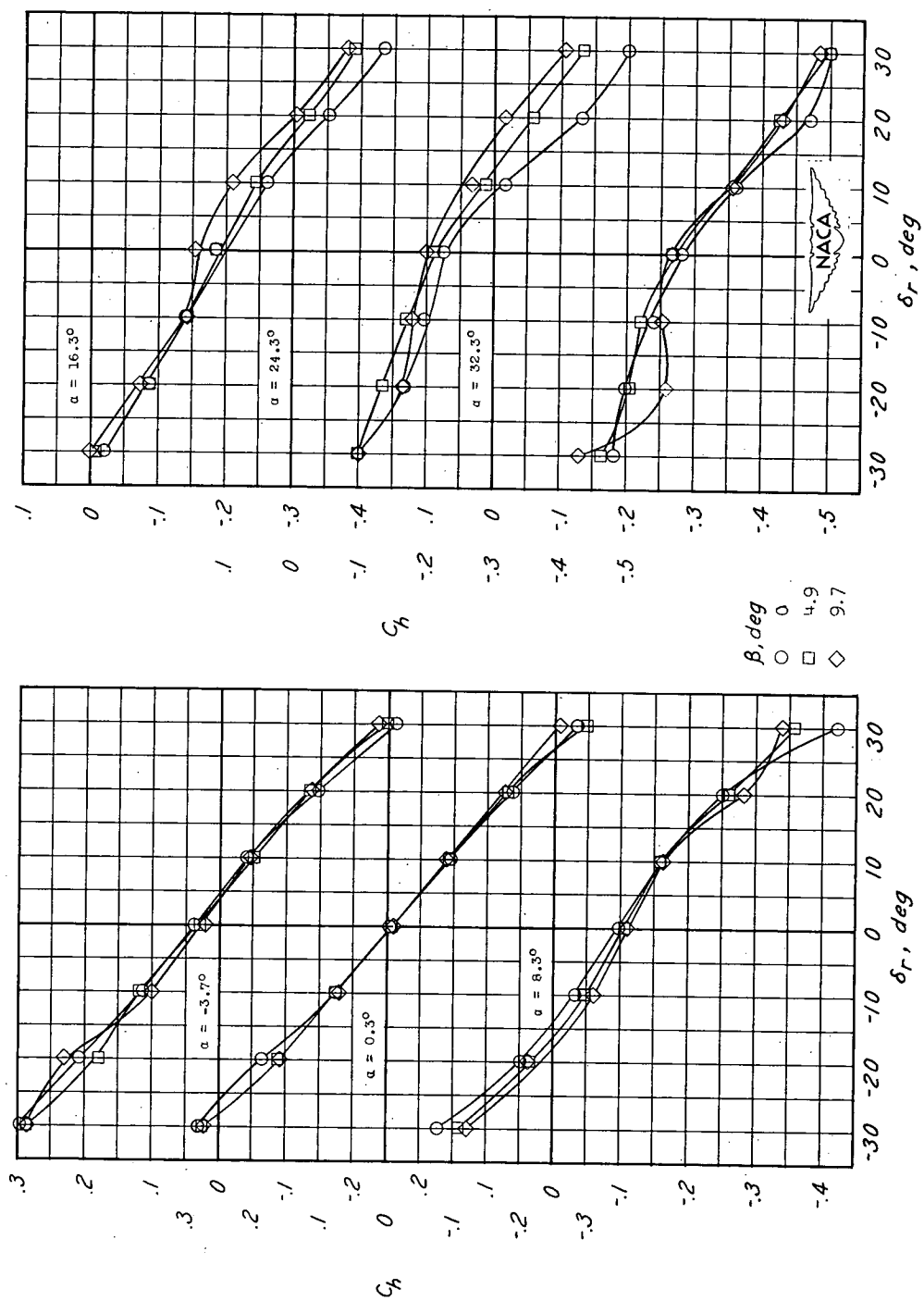

(a) Right aileron, model without nacelles.

Figure 10.- Variation of aileron hinge-moment coefficient with aileron deflection at several angles of sideslip.

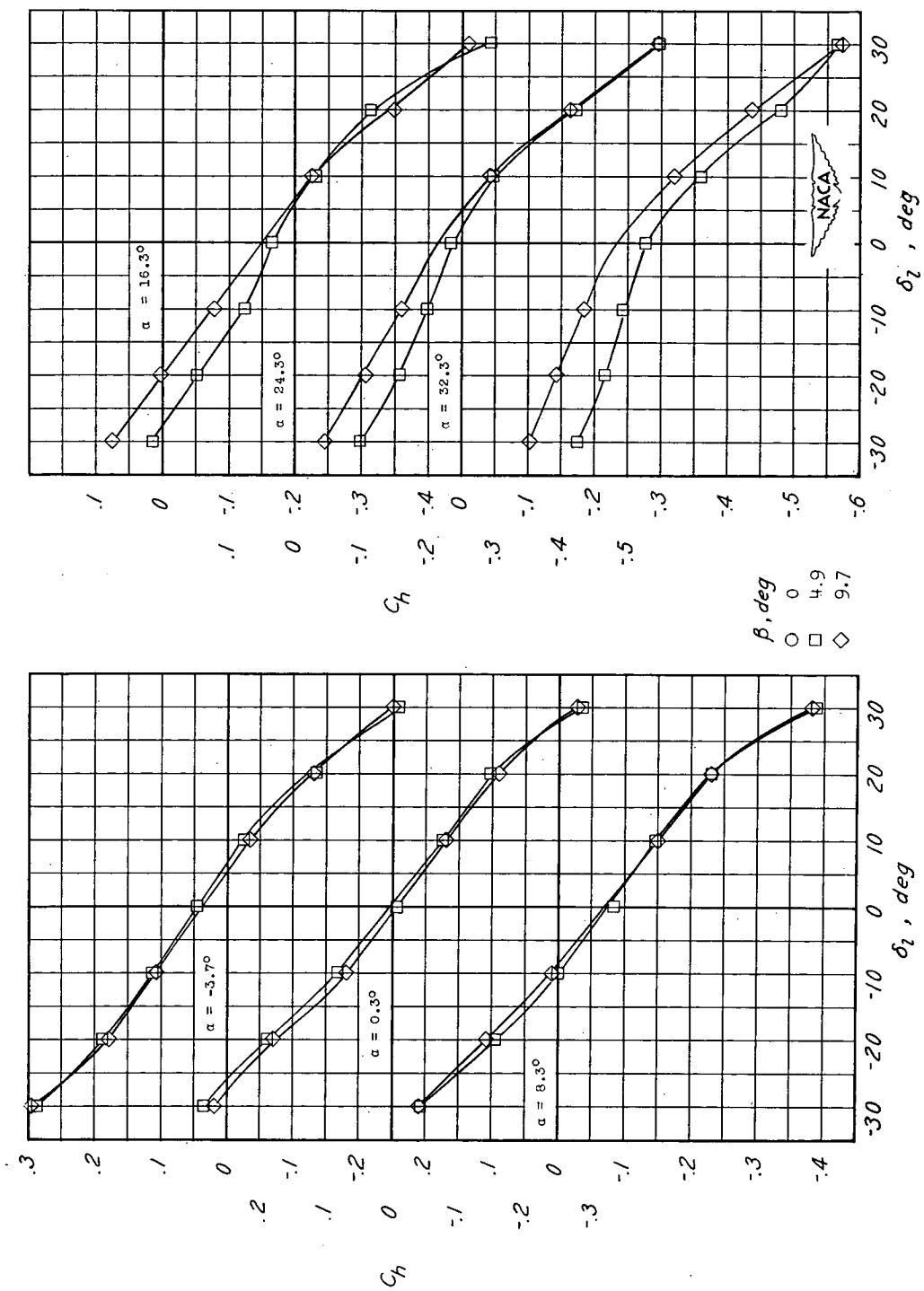

(b) Left aileron, model without nacelles.

Figure 10.- Continued.

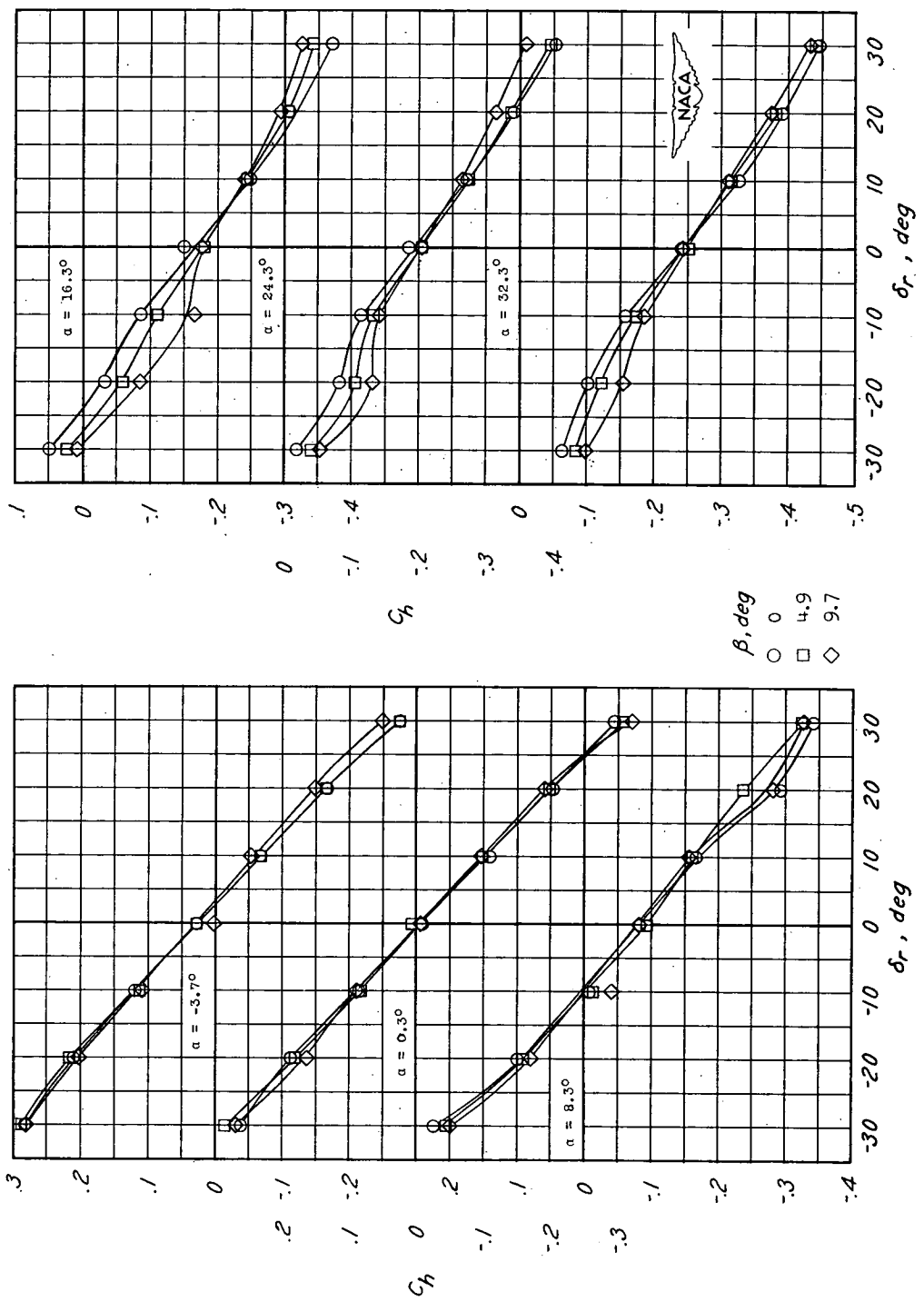

(c) Right aileron, model with nacelles.

Figure 10.- Continued.

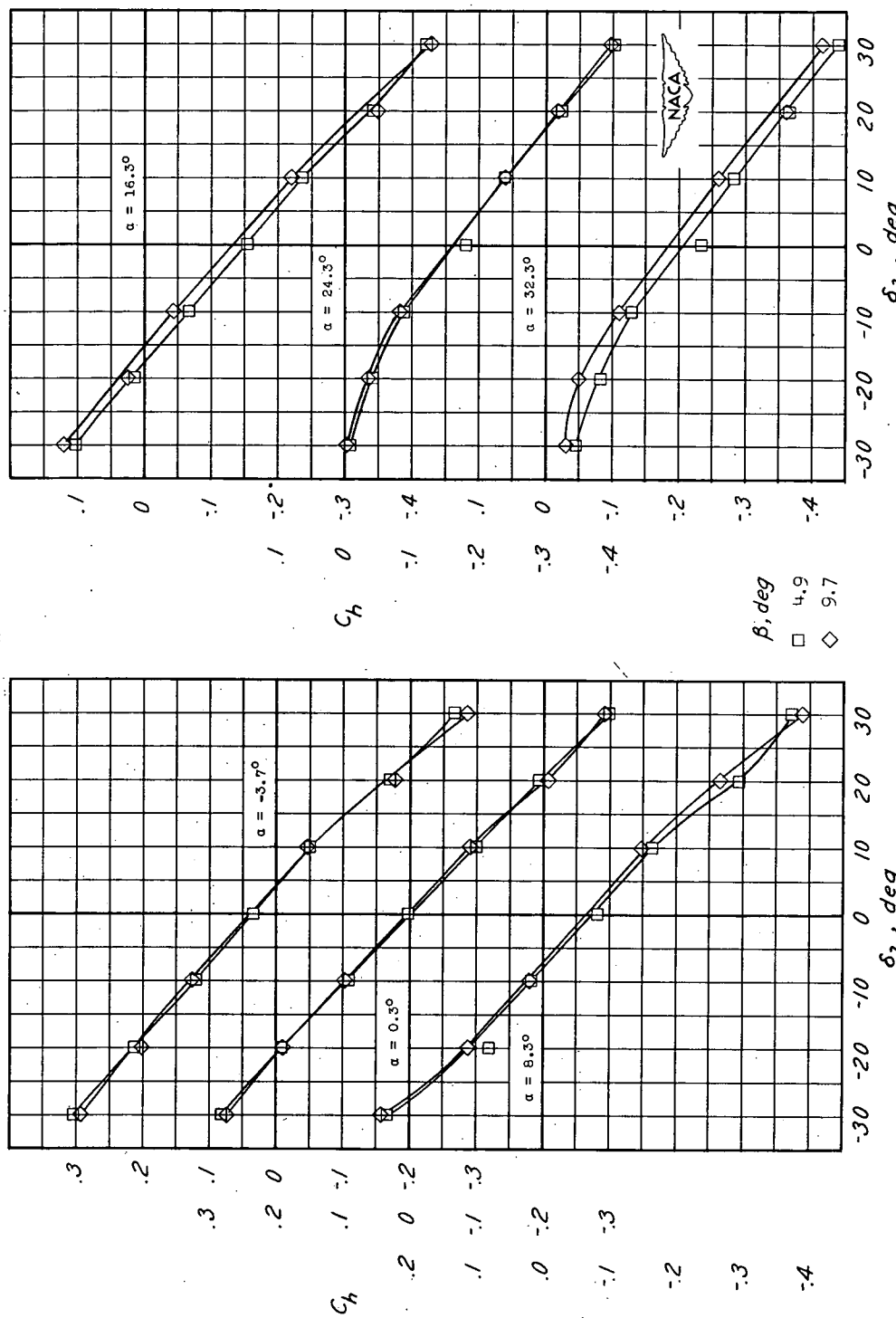

(d) Left aileron, model with nacelles.

Figure 10.- Concluded.

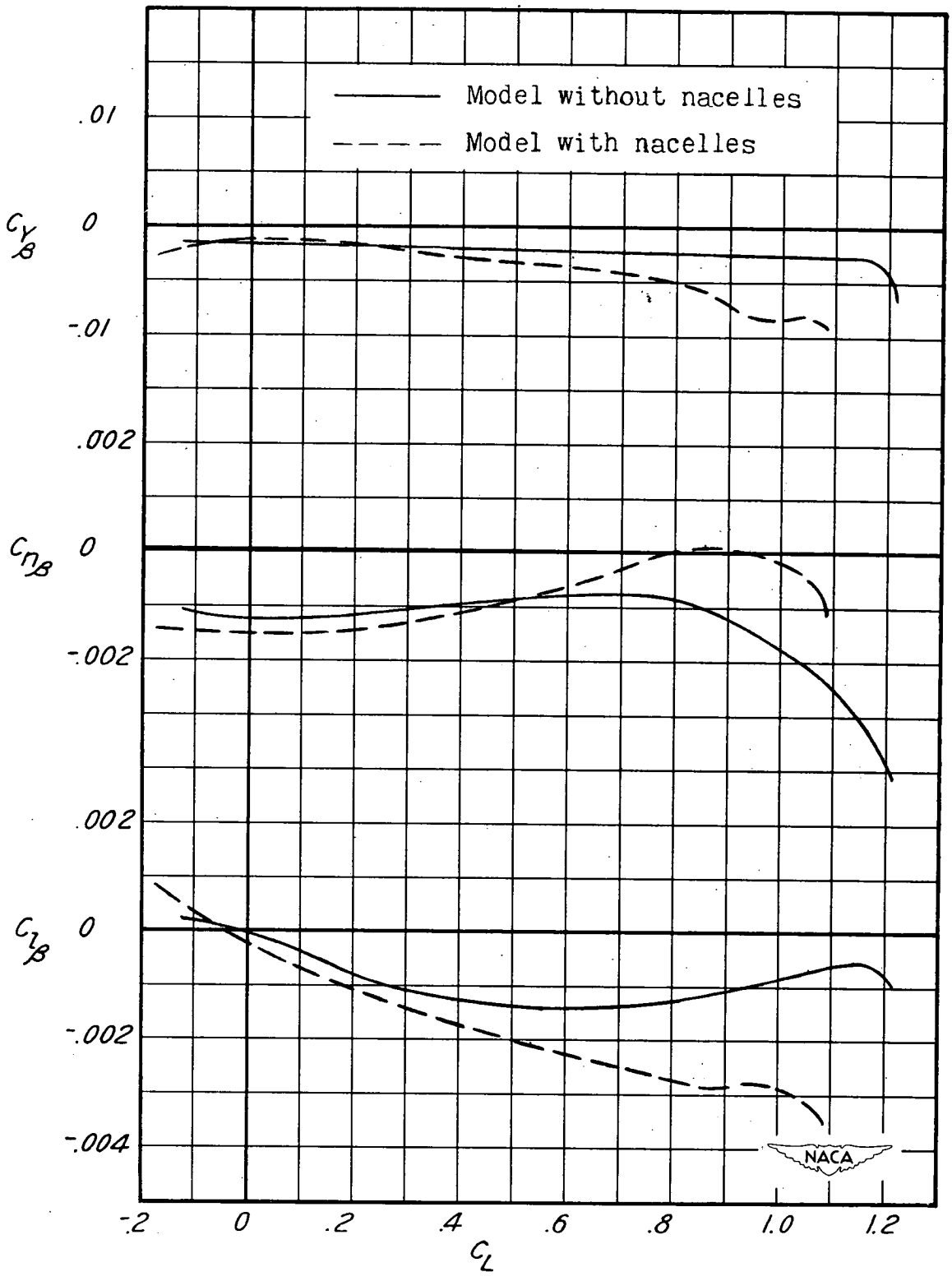

Figure 11.- Variation of the lateral and directional parameters with lift coefficient.

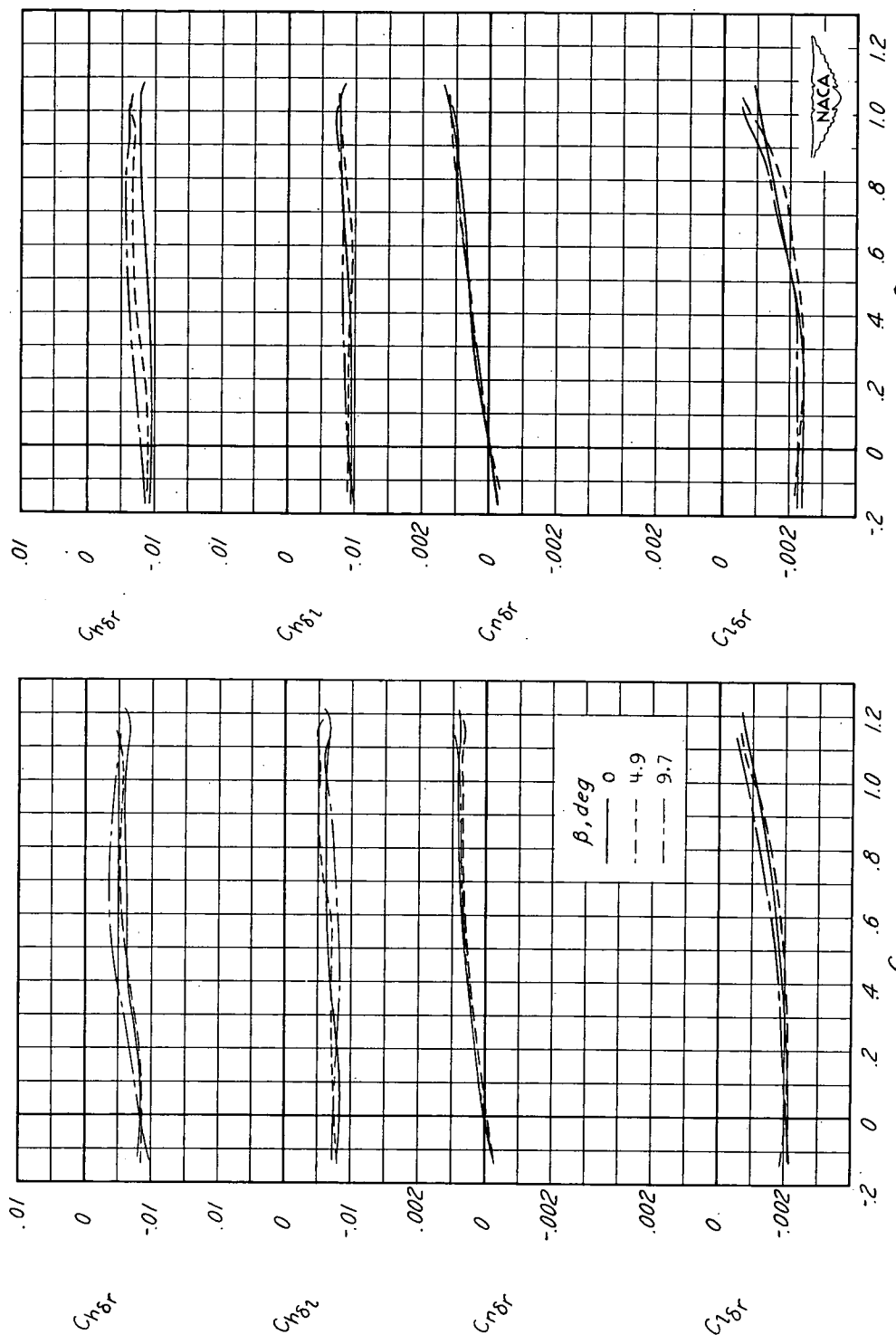

Figure 12.- Variation of the control and hinge-moment parameters with lift coefficient at several angles of sideslip.

NACA-Langley - 8-21-53 - 325